

A Compact Monitoring Circuit to Accurately Extract Fabrication Deviation in Silicon Waveguides

Tsuyoshi Horikawa, Hideaki Okayama, Yosuke Onawa, Daisuke Shimura,
Jun Ushida, Akemi Shiina, Tadashi Murao, and Hiroki Yaegashi

Photonics Electronics Technology Research Association (PETRA), 16-1 Onogawa, Tsukuba, Ibaraki, 305-8569, Japan, tsuyoshi.horikawa@petra-jp.org

Abstract Novel optical circuit with a microring resonator and polarization rotators was proposed for process control monitoring. The extraction method by TE and TM spectral analysis using the circuit showed sensitivity to sub-nm order fabrication deviations as well as robustness to measurement errors.

Introduction

In silicon-based photonic integrated circuits (Si-PIC), the waveguide defines the propagation path of signal light between optical functionalities and is also the basic structure of most wavelength filters. It has been reported that the fabrication deviation in the waveguides causes spectral changes in waveguide filters [1, 2]. It is, therefore, an important concern to ensure the reproducible manufacturing of the Si-PICs by establishing the methodology for in-line process control monitoring (PCM).

The extraction of width and height deviations in the wire-waveguides through spectral analysis using optical circuits containing Mach-Zehnder interferometers (MZI) [3] or microring resonators (MRR) [4-5] has been proposed as optical PCM methods. In our previous paper [5], the deviations of effective and group refractive indices for the lowest-order transverse electric (TE) propagation in each MRR were first evaluated from the variations in the resonant wavelength and free spectral range (FSR) measured for a large number of MRRs, and then the fabrication deviations were derived from the index deviations. Note that the measurement error for small FSR shifts determines the accuracy in the extraction of the fabrication deviations.

In this paper, we propose a suitable methodology to accurately extract the fabrication deviation. Here, we introduce a new compact monitoring circuit with an MRR and polarization rotators, which is designed for TE mode and transverse magnetic (TM) mode propagation. The main feature of the methodology is to extract fabrication parameters using the effective index change in TE and TM modes. This method is theoretically and experimentally demonstrated to enable more accurate parameter extraction for the wire-waveguide than the previous method [5]. Finally, we will discuss the applicability of this methodology as process control monitoring in manufacturing Si-PIC.

Characteristics of monitoring circuit

The monitoring circuit consisted of an MRR, two polarization rotators (PRs), and four grating couplers (GCs) (Fig. 1). As for the MRR, the ring radius and the gap between the ring and bus waveguide were $5\ \mu\text{m}$ and $200\ \text{nm}$, respectively. The width for the wire-waveguide in the MRR and bus line was $350\ \text{nm}$. Table 1 summarizes the design parameters for TE and TM propagation in the waveguide. The PR contained the directional coupling and rotation segments. The gap between the main and side arms in the coupling segment was kept to be $200\ \text{nm}$ and the side arm tip was inversely tapered with a tip width of $170\ \text{nm}$. The TE mode propagating light from the side arm transitions into the main arm in the coupling segment and changes the polarization mode from TE to TM in the rotation segment. The GC was designed to optically couple TE mode propagating light in the waveguide with the probing fibers. Different GC pairs were selected for TE and TM mode measurement, as shown in Fig. 1.

The monitoring circuit was fabricated by using PETRA Si-PIC platform technology based on 40-nm node CMOS technology with 300-mm -diameter SOI [6, 7]. The thicknesses of SOI and BOX were $200\ \text{nm}$ and $2\ \mu\text{m}$, respectively. TE and TM drop-port spectra of MRR in the fabricated monitoring circuit were observed at the temperature of $25\pm 0.1\ ^\circ\text{C}$ (Fig. 2). In both TE and TM spectra, three distinct peaks appeared within

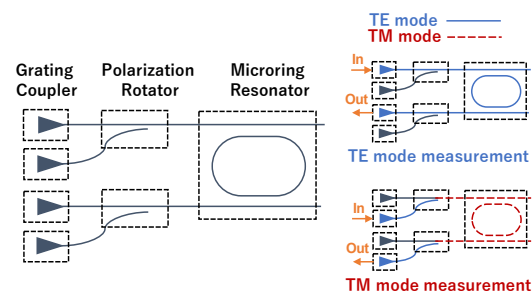


Fig. 1: Schematic for the configuration of the circuit (left). Optical paths in the circuit for TE mode (upper right) and TM mode (lower right) measurement.

Tab. 1: Design parameters of the waveguide for MMR in the monitoring circuit. The refractive indices and their partial derivatives were calculated for the wavelength of 1310 nm by a finite element method.

Width, W	350 nm		W	H
Height, H	200 nm	$\frac{\partial n_{e,TE}}{\partial X}$	0.003174	0.004061
$n_{e,TE}$	2.361	$\frac{\partial n_{g,TE}}{\partial X}$	-0.002853	0.000988
$n_{g,TE}$	4.439	$\frac{\partial n_{e,TM}}{\partial X}$	0.001298	0.008568
$n_{e,TM}$	1.838	$\frac{\partial n_{g,TM}}{\partial X}$	0.003641	0.031809
$n_{g,TM}$	4.136			

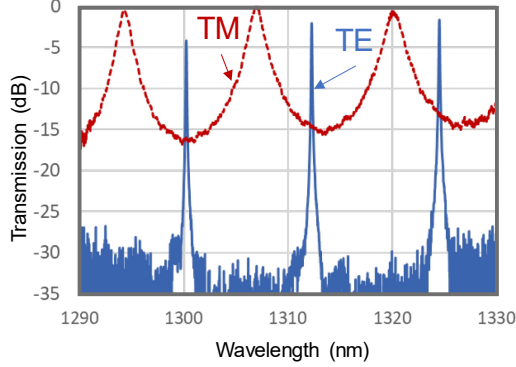


Fig. 2: Transmission spectra from MRR drop port of the monitoring circuit for TE mode (blue solid line) and TM mode (red dotted line) propagation

the observed wavelength range. The FWHM for TM peaks was larger than that for TE peaks, which shows the stronger coupling between the ring and bus line for TM mode.

Figure 3 shows TE and TM drop port spectra for 64 circuits on a single wafer. The resonant wavelength range for these MRRs is 9 nm for TE and 5 nm for TM, respectively. Note that, in Fig. 2 and 3, there are no additional peaks corresponding to crosstalk between TE and TM modes. This means that the polarization rotator has a very high conversion ratio and there is little conversion during propagation through the MRR.

Extraction of fabrication deviation

The extraction of the fabrication deviation using the variation in resonance frequency for TE and TM mode resonances in microdisk resonators was reported by W. A. Zortman et al. [8]. Here, we rewrite their extraction procedure for MRR in this study, using the deviation in the refractive indices, $\Delta n_{e,TE}$ and $\Delta n_{e,TM}$. Given small changes in waveguide width and height, ΔW and ΔH , the change in $n_{e,TE}$ and $n_{e,TM}$ can be written using ΔW , ΔH and a coefficient matrix M in the form,

$$\begin{bmatrix} \Delta n_{e,TE} \\ \Delta n_{e,TM} \end{bmatrix} \approx \begin{bmatrix} \frac{\partial n_{e,TE}}{\partial W} & \frac{\partial n_{e,TE}}{\partial H} \\ \frac{\partial n_{e,TM}}{\partial W} & \frac{\partial n_{e,TM}}{\partial H} \end{bmatrix} \begin{bmatrix} \Delta W \\ \Delta H \end{bmatrix} = M \begin{bmatrix} \Delta W \\ \Delta H \end{bmatrix}, \quad (1)$$

where Δn_e can be expressed by the resonance wavelength shift $\Delta \lambda_{res}$ in the form $\Delta n_e =$

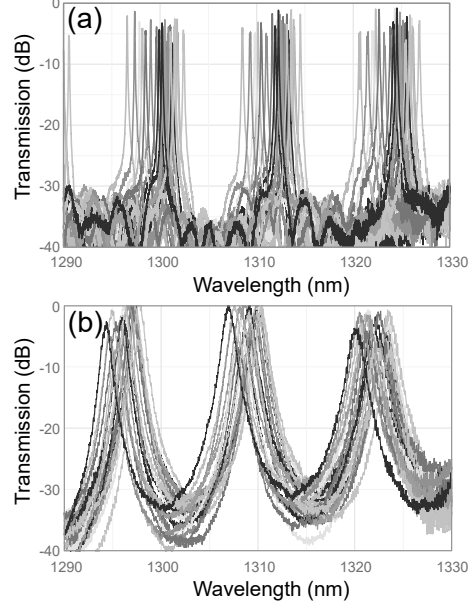


Fig. 3: The drop port spectra for TE (a) and TM (b) mode propagation observed for 64 MRRs on a single wafer.

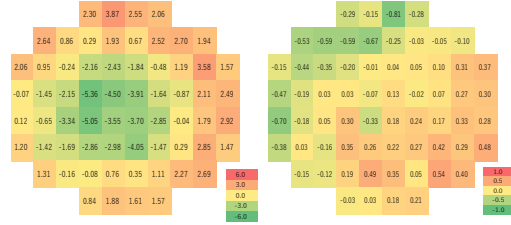


Fig. 4: Contour maps for the deviations of the waveguide width (a) and height (b) extracted by using the monitoring circuits fabricated on a single 300-mm SOI wafer.

$n_g \Delta \lambda_{res} / \lambda_{res}$. By the inverse matrix calculation for Eq. (1), ΔW and ΔH for each circuit can be derived. Note that the above extraction procedure is the same as previously reported [5] except that $\Delta n_{e,TM}$ is used instead of $\Delta n_{g,TE}$.

Figure 4 shows contour plots of the waveguide width and height deviations extracted for 64 monitoring circuits fabricated on a single 300-mm SOI wafer. The numerical values of partial derivatives of $n_{e,TE}$ and $n_{e,TM}$ to W and H in Table 1 were used for the calculation. The obtained width plot well reproduced the previous width distribution measured by CD-SEM for a wafer fabricated using the same process [5]. Also, the height map well reflected initial SOI thickness distribution for a 300-mm SOI wafer with sub-nm order accuracy.

Accuracy and robustness of this method

In the inverse matrix calculation based on Eq. (1), the determinant of the coefficient matrix, $|M|$ strongly influences the accuracy of extracted fabrication deviation. The value of $|M|$ can be expressed as the area of a parallelogram defined by two red vectors in Fig. 5, where the change in $n_{e,TE}$ and $n_{e,TM}$ induced by the increase of 1 nm

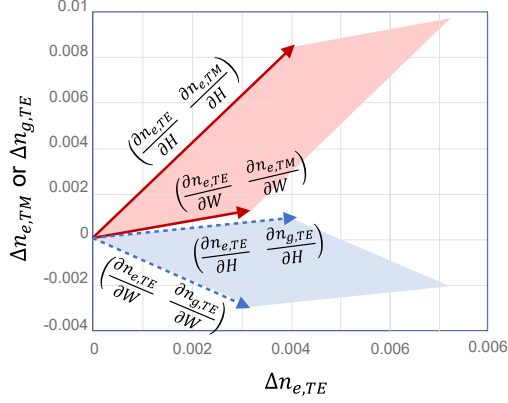


Fig. 5: The refractive index changes induced by the increase of 1 nm in waveguide width and height. Red vectors express the change in $n_{e,TE}$ and $n_{e,TM}$, and blue vectors express the change in $n_{e,TE}$ and $n_{g,TE}$.

in the waveguide width and height was expressed by the red vectors. Compared with the previous method using $n_{e,TE}$ and $n_{e,TM}$ (blue vectors in Fig. 5), the proposed method showed 48% larger value of $|M|$, which means the method provides superior accuracy than the previous method.

Next, we examine the propagation of the measurement error. Suppose that the measurement error of resonant wavelength $\delta(\Delta\lambda_{res})$ mainly causes the error in the deviation of the refractive indices $\delta(\Delta n_e)$, it should be expressed in the form,

$$\delta(\Delta n_e) \approx n_g \frac{\delta(\Delta\lambda_{res})}{\lambda_{res}}, \quad (2)$$

Combining Eqs. (1), (2), and the numerical values of coefficients in Table 1, the error propagation to the fabrication deviation is derived as follows,

$$\delta(\Delta W[\text{nm}]) \sim 1.9 \times 10^3 \frac{\delta(\Delta\lambda_{res})}{\lambda_{res}} = 1.4 \delta(\Delta\lambda_{res}[\text{nm}]), \quad (3)$$

$$\delta(\Delta H[\text{nm}]) \sim 0.7 \times 10^3 \frac{\delta(\Delta\lambda_{res})}{\lambda_{res}} = 0.5 \delta(\Delta\lambda_{res}[\text{nm}]), \quad (4)$$

where we supposed that $\delta(\Delta\lambda_{res})$ for TE and TM measurements is the same value for simplicity. As for the extraction using $\Delta n_{e,TE}$ and $\Delta n_{g,TE}$, the error in fabrication deviation is mainly caused by $\delta(\Delta LER)$. In such case, the error in deviation is estimated using the equation,

$$\delta(\Delta W[\text{nm}]) \sim 1.2 \times 10^3 \frac{\delta(\Delta LER)}{LER} = 102 \delta(\Delta LER[\text{nm}]), \quad (5)$$

$$\delta(\Delta H[\text{nm}]) \sim 0.9 \times 10^3 \frac{\delta(\Delta LER)}{LER} = 74 \delta(\Delta LER[\text{nm}]). \quad (6)$$

From the repetition of TE & TM measurement, the measurement errors for $\delta(\Delta\lambda_{res})$ and $\delta(\Delta LER)$ were estimated to be around 1 pm in 1σ under our measurement condition, as shown in Fig. 6. Hence, it is clear that, comparing Eqs. (3), (4) with Eqs. (5) and (6), the proposed method shows negligible error propagation from measurement and, thus, is much more robust to

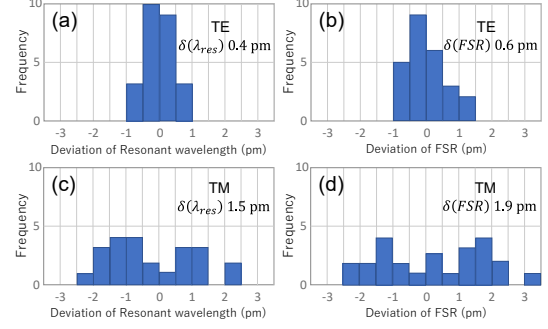


Fig. 6: The frequency histogram for the deviation of the resonant wavelength and FSR in 25 repetition of TE measurement for the same device. (a) wavelength deviation for TE, (b) FSR deviation for TE, (c) wavelength deviation for TM, and (d) FSR deviation for TM.

measurement error than the previous method.

By using the proposed monitoring circuit and wafer-level probing system, in-line optical PCM data can be easily obtained, and the methodology described here can provide accurate fabrication deviation using these data. Thus, we think that the monitoring circuit and methodology in this paper is a best couple to extract fabrication deviation. However, the validation of extracted results will be remained as a concern, because any other conventional PCM techniques cannot provide enough accuracy. The PCM system using other optical devices may provide a practical solution.

Note that the monitoring circuit in this study should be applicable to the parameter extraction for the rib-waveguide. There are three key physical parameters of the core width, core height, and etching depth in the rib-waveguide. The spectral analysis for the monitoring circuit provides the deviations of four independent refractive indices, $\Delta n_{e,TE}$, $\Delta n_{g,TE}$, $\Delta n_{e,TM}$ and $\Delta n_{g,TM}$, which will enable to consistently extract the above three physical parameters. The measurement error of group indices should determine extraction accuracy in such case.

Conclusions

We presented a monitoring circuit with an MRR and polarization rotators, which is designed for TE and TM mode propagation, and proposed the methodology using the circuit to extract the deviation of fabrication parameters from effective index change in TE and TM mode. The proposed method was shown to have a good sensitivity to sub-nm order fabrication deviations as well as robustness to measurement errors.

Acknowledgements

This research is based on results obtained from a project, JPNP13004, commissioned by the New Energy and Industrial Technology Development Organization (NEDO).

References

- [1] S. H. Jeong et al., "Low-loss, flat-topped and spectrally uniform silicon nanowire-based 5th-order CROW fabricated by ArF-immersion lithography process on a 300-mm SOI wafer," *Opt. Express*, vol. 21, no. 25, pp. 30163–30174, Dec. 2013.
- [2] H. Okayama et al., "Si wire array waveguide grating with parallel star coupler configuration fabricated by ArF excimer immersion lithography," *Electron. Lett.*, vol. 49, no. 6, pp. 410–411, Mar. 2013.
- [3] S. Dwivedi et al., "Experimental extraction of effective refractive index and thermo-optic coefficients of silicon-on-insulator waveguides using interferometers," *J. Lighw. Technol.* vol. 33, pp. 4471–4477, Nov. 2015.
- [4] Z. Lu et al., "Performance prediction for silicon photonics integrated circuits with layout-dependent correlated manufacturing variability," *Opt. Express*, vol. 25, no. 9, pp. 9712–9733, May 2017.
- [5] T. Horikawa et al., "Resonant wavelength variation modelling for microring resonators based on fabrication deviation analysis," in *Proc. 43rd Eur. Conf. Opt. Commun.*, Gothenburg, Sweden, Sep. 2017.
- [6] T. Horikawa et al., "A 300-mm silicon photonics platform for large-scale device integration," *IEEE J. Sel. Top. Quantum Electron.*, vol. 24, no. 4, Mar. 2018.
- [7] T. Mogami et al., "1.2 Tbps/cm² enabling silicon photonics IC technology based on 40-nm generation platform," *J. Lighw. Technol.* vol. 36, pp. 4701–4712, Oct. 2018.
- [8] W. A. Zortman et al., "Silicon photonics manufacturing," *Opt. Express*, vol. 18, no. 23, pp. 23598–23607, Nov. 2010.